

# Traffic noise spectrum analysis: Dynamic modeling vs. experimental observations

A. Can, L. Leclercq<sup>\*</sup>, J. Lelong, D. Botteldooren

Université de Lyon, INRETS/ENTPE, LICIT, Rue Maurice Audin, 69518 Vaulx-en-Velin Cedex, France

## ARTICLE INFO

### Article history:

Received 4 January 2010

Received in revised form 31 March 2010

Accepted 2 April 2010

Available online 14 May 2010

### Keywords:

Traffic representations

Noise spectrum

Urban traffic noise

Dynamic noise assessment

## ABSTRACT

This paper compares two traffic representations for the assessment of urban noise frequency spectrum: (i) a static one, based on mean vehicle speeds and flow rates, (ii) a dynamic one, which considers vehicle interactions along the network. The two representations are compared on their suitability to match real on-field noise levels, recorded on a three lane quite busy street. Representation (i) fails in reproducing spectra envelopes that correspond to this site. In particular, it underestimates low frequencies, what can conceal the real impact of traffic flow on urban sound quality. Representation (ii) greatly improves estimation. It guarantees accurate environmental noise assessment, since it reproduces all traffic situations that are encountered in the site. Moreover, its 1s-based structure allows for the evaluation of spectra variations, with a good accuracy.

© 2010 Elsevier Ltd. All rights reserved.

## 1. Introduction

The frequency spectra highly influence sound quality [1]. In particular, low frequencies due to road traffic flow deteriorate urban soundscape [2,3]. High frequencies which can emerge from traffic noise also increase annoyance [1]. Moreover, frequency variations play an important role in sound quality [4]. Thus traffic noise prediction models should take frequency spectra into account to precisely assess the influence of traffic flow on noise quality in urban area.

The modeling chain for noise estimation is made of four steps: (i) a traffic model that estimates the characteristics of traffic flow (speeds, flow rates, etc.), (ii) a noise emission model that gives the noise power level  $L_w$  emitted by vehicles, (iii) a sound propagation model that gives the sound pressure level  $L_p$  at a receiver, and (iv) the calculation of noise indicators to highlight sound characteristics. Each of those four steps should efficiently reproduce spectral contents to describe characteristics of urban traffic noise.

Large efforts have been invested for years to improve steps (ii) and (iii). Current noise emission models give the power level emitted by vehicles for each 1/3 octave bandwidths according to their class (light vehicles, trucks, etc.), speed, and acceleration (cruising mode [5] or acceleration range [6] depending on the models). Sound propagation models usually consider noise attenuation for each 1/3 octave or each octave bandwidth. Moreover, the effects of noise reducers (noise barriers, road surface, etc.) are usually given in terms of an emitted spectrum [7], or in terms of a given vehicle speed [8], knowing that those performances highly depend

on frequency. For example, noise barriers offer substantial noise attenuation for high frequencies but hardly stop low frequencies. Moreover, the influence of their shape on efficiency depends on frequency [9]. Hence, the estimation of the noise spectrum due to the whole traffic stream is crucial to guarantee an accurate estimation of the whole modeling chain.

Nevertheless, for urban traffic noise assessment, studies often restrict step (i) to a *static* traffic representation which assumes a given mean vehicle speed. This could annihilate the accuracy offered by noise emission and sound propagation models. Recent developments on *dynamic* noise models make it possible to consider the impacts of vehicle kinematics on noise pattern [10–12]. Those models are based on a dynamic traffic model that gives vehicle kinematics at each time step (typically 1s), coupled to noise emission and sound propagation models. Ref. [13] has shown through comparisons with measurements that dynamic models outperform static ones for  $L_{Aeq}$  estimation. They also allow for estimating the 1s-noise levels evolution, and thus noise dynamics [14].

This paper will extend the comparison of both approaches by focusing on spectra aspects. The aim is to: (i) show the limits of the static approach for frequency spectrum assessment, (ii) prove that the dynamic approach improves spectrum estimation and allows for the estimation of acoustical indicators that reflect the spectrum content of traffic noise. Both approaches will be applied on a three lanes quite busy street. They are compared on their suitability to reveal the characteristics of the noise spectrum spectra recorded at four different points, which correspond to four real traffic situations: in front of a traffic signal, down to a traffic signal, close to a bus station, and away from the main street.

The modeling chain and the acoustical indicators used for comparison are presented in Section 2. Section 3 is devoted to

<sup>\*</sup> Corresponding author. Tel.: +33 4 72047716; fax: +33 4 72047712.  
E-mail address: [leclercq@entpe.fr](mailto:leclercq@entpe.fr) (L. Leclercq).

the comparison of the two approaches. Finally, Section 4 points out the key elements to offer a valuable tool for the assessment of noise impact of urban traffic policies.

## 2. Methodology

### 2.1. Experimentation

The experiment consists in traffic and acoustic measurements, carried out from 15.30 h to 17.30 h on a weekday, in the Cours Lafayette (Lyon, France). It is explained in details in [13]. The site is a one-way three-lane urban corridor (the shoulder lane is shared by buses and passenger cars) with five signalized intersections. The street is U-shaped with 5-floor buildings. It is quite busy, with about 1400 veh/h during the experiment. Nevertheless, these flow rates are too low to observe residual congestion during the experiment. The traffic signals are coordinated through a green wave: a vehicle that arrives at the first intersection at its free-flow speed faces a green signal at the next traffic light. Detailed characteristics of traffic signals are given in Fig. 1.

The recorded traffic data is the number of vehicles per cycle at each intersection and for each movement, and the precise bus trajectories (including stopping times at bus stations). Acoustic recordings are the 1s-evolution of the octave bandwidth sound spectra, for the selected points. Points for noise levels measurements are located on the curb, at a distance of 2.5 m from the building. The four selected points are typical of urban situations:

- in front of a bus station downstream of a traffic signal ( $P_1$ ),
- in front of a traffic signal ( $P_2$ ),

- down to a traffic signal ( $P_3$ ) and
- set back from the major street (the flow rate on the perpendicular street is 250 veh/h).

Measurement points are 2 m-high. Their exact location is given in Fig. 1.

### 2.2. Calculation process

#### 2.2.1. Noise estimation

Each acoustic value  $L_x$  is an eight element vector, which corresponds to the values of the octave bands with center frequencies from 63 Hz to 8 kHz:  $\{L_{x,63}; \dots; L_{x,8k}\}$ . Emission and propagation are computed for each octave. Each lane of the traffic network is divided into noise cells  $i$ . Noise cells are between 9 m and 18 m length since this size is suitable for dynamic noise prediction [15]. Cell lengths vary from one link to another due to differences in link sizes, but have the same size within a given traffic link. Noise cells are defined by their sound power level  $L_{w,i}$ , which is calculated by gathering the emissions of all vehicles present inside the cell. The Harmonoise model is used to predict the sound power level  $L_{w,k}$  of one given vehicle  $k$ , in terms of its speed  $v_k$  and its acceleration  $a_k$  [6]; see Fig. 2. The way those variables are obtained depends on the traffic flow representation included into the noise prediction model (see Section 2.2.2).

The contribution  $L_{p,i}$  of each cell for a receiver  $P$  is then determined thanks to the propagation model NMPB-routes-96 implemented in Mithra [16], which gives the sound attenuation from  $i$  to  $P$ . Finally, the sound pressure level  $L_p$  at  $P$  (which is also a eight element vector) is the sum of the contributions of each cell:

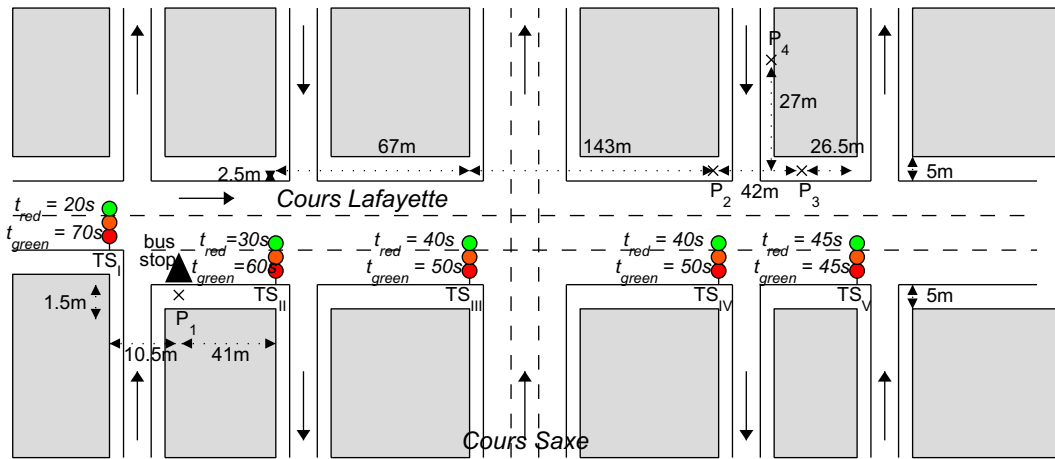


Fig. 1. Experimental site. Position of traffic signals TS and their green time  $t_g$  and red time  $t_r$  durations.

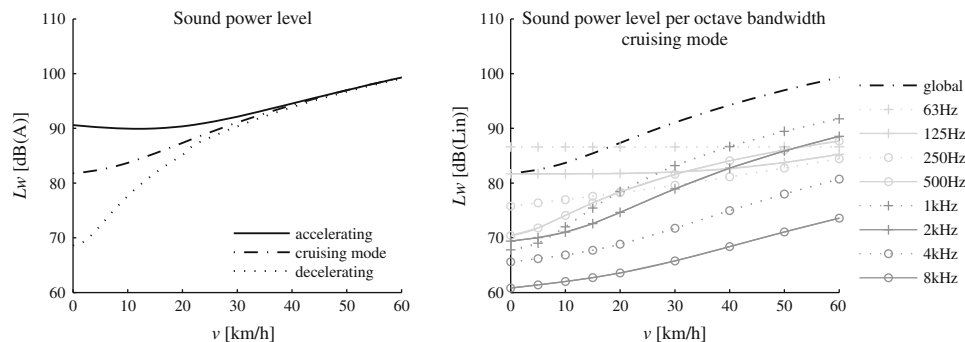


Fig. 2. Noise emission laws for light vehicles: accelerating ( $a = 0.8 \text{ m/s}^2$ ), cruising ( $a = 0 \text{ m/s}^2$ ) or decelerating ( $a = -3 \text{ m/s}^2$ ).

$$L_p = 10 \log \left( \sum_{i \in \text{cell}} 10^{\frac{L_{p,i}}{10}} \right) \quad (1)$$

### 2.2.2. Traffic flow representations

The static and the dynamic models have a different approach and resolution. The dynamic model allows for  $L_{p,1s}$  evolution estimation since it describes the evolution of traffic variables in time. The static model only allows for the  $L_{p,2h}$  estimation, since it considers mean values for traffic variables over the 2 h simulation period. Hence, only the former allows for specific descriptors calculation, based on  $L_{p,1s}$  values.

**2.2.2.1. Static representation.** Two classes  $c$  of vehicles are considered: light vehicles  $lv$  and buses  $bus$ , defined by their flow rates  $Q^{lv}$  and  $Q^{bus}$ . Linear sound power level  $L_W^c$  of a given cell is deduced from the mean speed  $v^c$ , acceleration  $a^c$  and flow rate  $Q^c$  on the cell:

$$L_W^c = L_W(v^c, a^c) + 10 \log \left( \frac{Q^c}{v^c} \right), \text{ with } c = \{lv, bus\} \quad (2)$$

No acceleration or deceleration zones are considered in usual static models: vehicles are supposed to pass through intersections without stopping. Hence,  $a^c = 0$  whatever the cell is. Finally, the noise power level  $L_W$  of the cell is the acoustical sum  $\oplus$  of the emissions  $L_W^{lv}$  and  $L_W^{bus}$  of the cell:

$$L_W = L_W^{lv} \oplus L_W^{bus} \quad (3)$$

**2.2.2.2. Dynamic representation.** Dynamic traffic models aim at predicting how key traffic variables evolve along the network. The model used in this study is SYMUVIA<sup>1</sup>, which is based upon a detailed and individualized vehicle representation. SYMUVIA is a component of the noise simulation package SYMUBRUIT that dynamically estimates noise in urban area [13,17]. It gives position  $x_k(t)$ , speed  $v_k(t)$  and acceleration  $a_k(t)$  of each vehicle  $k$  on the network at each time step (usually about 1s). Motion of vehicles on the network is governed by three parameters: the maximal speed  $u$  reached when traffic is free, the wave speed  $w$  at which a starting wave<sup>2</sup> spills back on the network (thus  $w$  is negative), and the minimum spacing  $s_{\min}$  between two vehicles, observed when vehicles are stopped for example at a traffic signal. Position of a vehicle  $k$  at the next time step  $x_k(t + \Delta t)$  is the minimum between the position it is willing to reach when traffic is free and the position it cannot overpass when traffic is congested, that is as soon as it is unable to reach the position he would reach if traffic were free. The time-step is fixed to  $\Delta t = -s_{\min}/w$  to have a numerical scheme that exactly matches analytical solutions, and avoids numerical viscosity. Then:

$$x_k(t + \Delta t) = \min \left( \underbrace{x_k(t) + u\Delta t}_{\text{position when traffic is free}}, \underbrace{x_{k-1}(t) - s_{\min}}_{\text{position when traffic is congested}} \right). \quad (4)$$

Speed  $v_k(t)$  and acceleration  $a_k(t)$  are then deduced from positions  $x_k(t)$  and  $x_k(t + \Delta t)$ . Noise power level  $L_{W,k}(t)$  of a vehicle is then calculated from its speed and acceleration at  $t$ . Finally, the noise power level  $L_{W,i}(t)$  of a cell  $i$  is the acoustical sum of noise emissions of vehicles on the cell at  $t$ :

$$L_{W,i}(t) = 10 \log \left( \sum_{k \in i} 10^{\frac{L_{W,k}(t)}{10}} \right), \quad (5)$$

where  $l_i$  is the length of the cell.

The model has been refined to take into account the bounded acceleration of vehicles [18], the influence of slow motion of buses [19], the lane-changing phenomena [20], and conflicts at junctions [21,22].

**2.2.2.3. Calibration.** Models have been calibrated to fit on-field measurements. The flow rates used for the simulations are the ones measured during the experiment (see Section 2.1). Traffic flow parameters are the wave speed  $w = -3.33$  m/s, the minimum spacing  $s_{\min} = 5$  m, and the maximal speed  $u$ . The maximal speed of light vehicles depends on the location on the network:  $u_1 = 17$  m/s at the beginning of the Cours Lafayette (up to the second intersection),  $u_2 = 15$  m/s at the end of the Cours Lafayette (after the second intersection), and  $u_3 = 10$  m/s on the crossing roads. The average acceleration rate is  $a = 0.8$  m/s<sup>2</sup>. The maximal speed of buses is  $u_{bus} = 10$  m/s. Finally, the background noise is taken into account by adding a constant level value afterward, calibrated on the minimum levels observed on field. It varies between 63 Hz and 8 kHz:  $L_{w,back} = \{60, 55, 50, 50, 45, 40, 35, 35\}$ , which corresponds to a global level of 51 dB(A).

### 2.2.3. Noise indicators

**2.2.3.1. Static indicators.** Static indicators are calculated for the 2 h period of the experiment, from the  $L_{p,2h}$  octave bandwidth values. They can be calculated by both static and dynamic models. They are:

- The sound level spectrum, which is the sound level  $L_{p,Bi}$  of each octave bandwidth ( $B_i$ ) from 63 Hz to 8 kHz.
- The spectrum is compared to Noise Rating curves. Those curves have been developed by the International organization of Standardization to rate noisiness [24]. Each  $x$  dB  $NR_x$  curve is built as follows: the value  $NR_{x,Bi}$  allocated to the octave bandwidth  $B_i$  is the sound level that a sound at the frequency  $B_i$  should have to be as noisy as a sound of  $x$  dB(Lin) at 1 kHz (thus  $NR_{x,1kHz} = x$ ).
- The Noise Rating value  $NR$  is also calculated from the sound spectrum at P. For each octave bandwidth  $B_i$ , a  $NR_x$  curve passes through the point  $L_{p,Bi}$ .  $NR$  is the maximum of the 8  $x$ ,  $B_i$  values that correspond to the 8 bandwidth. Hence this indicator takes emerging frequencies into account, since it reflects the most noisy octave bandwidth.
- The Spectrum Gravity Center SGC. This indicator makes an average of the sound power frequency spectra. Thus it approximates the “averaged pitch” of the sound. It is calculated as in [23]:

$$SGC = \frac{\sum_i B_i * 10^{\frac{L_i}{10}}}{\sum_i 10^{\frac{L_i}{10}}}, \text{ with } i \in \{63; \dots; 8k\}$$

where  $L_i$  is the sound level in dB(Lin) measured from each sound octave bandwidth ( $B_i$ ) from 63 Hz to 8 kHz.

**2.2.3.2. Dynamic indicators.** Dynamic indicators can only be calculated if the dynamic traffic model is used, since they are based on the evolution of the  $L_{p,1s}$  octave bandwidth values. They are:

- The «spectrum mean noise pattern». It is based on a previous study, which has demonstrated the strong periodicity of traffic noise on signalized junction streets [25]. It consists in the spectrum sound pressure levels evolution within a representative traffic signal cycle. The mean noise pattern is defined for each octave bandwidth as follows: (i) for each of the  $t_c$  instants  $t_i \in [0, t_c]$  the sample  $S_{ti}$  that contains the instants  $t \equiv t_i \pmod{t_c}$ <sup>3</sup> is constructed (hence there is  $t_c = 90$  samples

<sup>1</sup> SYMUVIA is a dynamic traffic simulation tool jointly developed by INRETS-ENTPE.

<sup>2</sup> A starting wave defines the mean time between two starts of consecutive vehicles at a green light.

<sup>3</sup> The symbol  $\equiv$  stands for modulo.

$S_{ti}$ , each one made of  $7200/t_c = 80$  elements), (ii) the median value of the elements of  $S_{ti}$  is calculated: it gives the value of the pattern at  $t_i$ . Finally, the «spectrum mean noise pattern» is the set of the eight mean noise patterns at each octave bandwidth  $B_i$ .

- The 1s and 10s SGC evolutions within a mean noise pattern. Both indicators are obtained by calculating SGC,  $t_i$  for each instant  $t_i$  of the mean noise pattern. They allow for quantifying pitch variations, which appear when vehicles speed varies and can play an important role on sound quality.

### 3. Results

#### 3.1. Static indicators

##### 3.1.1. Measurements

The observed sound spectra at the four points are shown in Fig. 3. They have some similarities; for instance the sound levels in dB(Lin) tend to decrease with the increasing frequency. The decrease between the 63 Hz and the 8 kHz sound levels reaches at least 20 dB for the four points. This can be explained by the road traffic noise spectrum, which contains more low than high frequencies (see Fig. 2). It results in a low Spectrum Gravity Centers (SGC) for the four points, between 266 Hz and 375 Hz (see Fig. 4).

Moreover, spectra show a peak at 1 kHz, which is mainly caused by the contact of tires on the road. It can be seen on Fig. 2 that this frequency is predominant for speeds above 40 km/h that is close to their free-flow speed. This peak causes high NR values (except for the point  $P_4$  that stands at further distance from the main road), since this indicator reflects the loudest octave bandwidth; see Section 2.2.3.2. Note that the 1 kHz peak is less pronounced at  $P_2$  (that is in front of the traffic signal), because lots of vehicles have to stop at this point before accelerating at low speeds for which the 1 kHz octave bandwidth is less energetic.

Finally, the sound levels at  $P_4$  sharply decrease with the frequency, mainly because of its specific location. This point is indeed less noisy than the others as it is set back from the street; but it still contains lots of low frequencies probably due to urban background

	NR				SGC			
	P <sub>1</sub>	P <sub>2</sub>	P <sub>3</sub>	P <sub>4</sub>	P <sub>1</sub>	P <sub>2</sub>	P <sub>3</sub>	P <sub>4</sub>
Measurements	70	67	67	62	376	288	315	267
Dynamic Model	70	66	66	57	383	353	379	288
Static Model	72	71	71	71	921	875	866	837

Fig. 4. Noise Ratings values and Sound Gravity Spectrum from Measurements and both static and dynamic models estimates.

noise. Those low frequencies explain why the SGC is lower at this point than for the other points. Moreover, noise decrease at this point is lesser than expected, which can be explained by the geometry of the site. Indeed, the perpendicular road, named “Rue Vendome”, is rather large and high for a secondary road, with a width of 25 m and a height of 20 m, leading to a height to width ratio of 0.8. This ratio allows for reverberation within the street, while the width of the street limits the screening effect.

##### 3.1.2. Static model

The spectra obtained by the static model tend to have the same envelope whatever the traffic situation is. They correspond to the noise emitted by a flow of vehicles moving at their free-flow speed. As the model cannot capture the feature of urban traffic flow (stops of vehicles at traffic signals, speed variations along the network due to traffic, etc.), it fails in reproducing the real spectra envelopes that correspond to each traffic situation. In particular, the low frequencies, which are mainly due to stops and slow vehicles, are underestimated by the static model. This results in a poor estimation of SGC, which stands at too high frequencies (errors exceed 100%), due to the speed overestimation. Moreover, the NR estimation is also biased by the speed overestimation: sound levels around 1 kHz are overestimated, so that NR is too high. Finally, the static model gives surprisingly high levels at  $P_4$ . Those high levels are due to the additional contribution of noise emitted at the intersection “Lafayette ∩ Vendome” and noise emitted within the

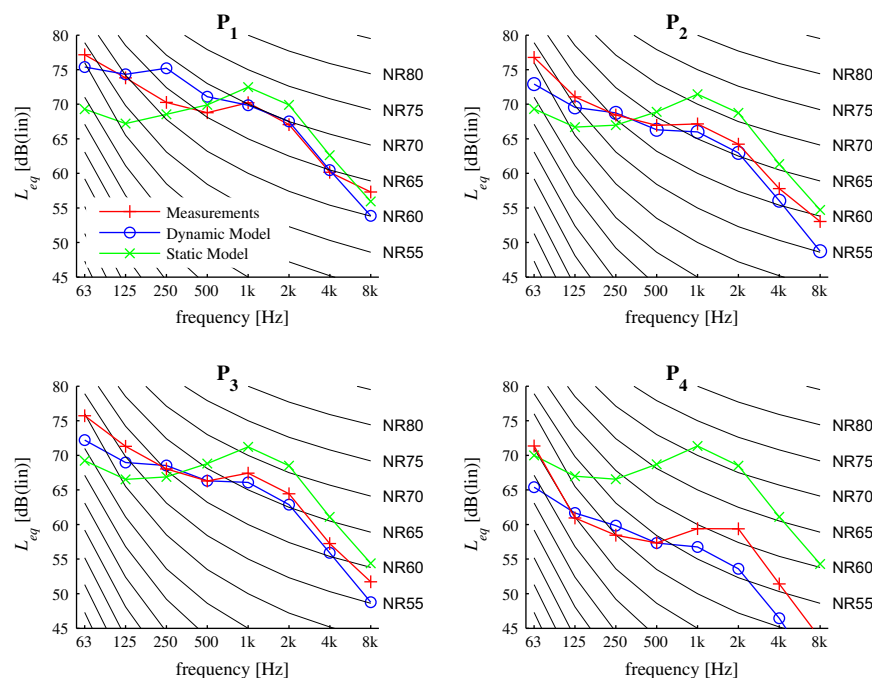


Fig. 3. Equivalent sound pressure level spectrum at the four measurement locations.

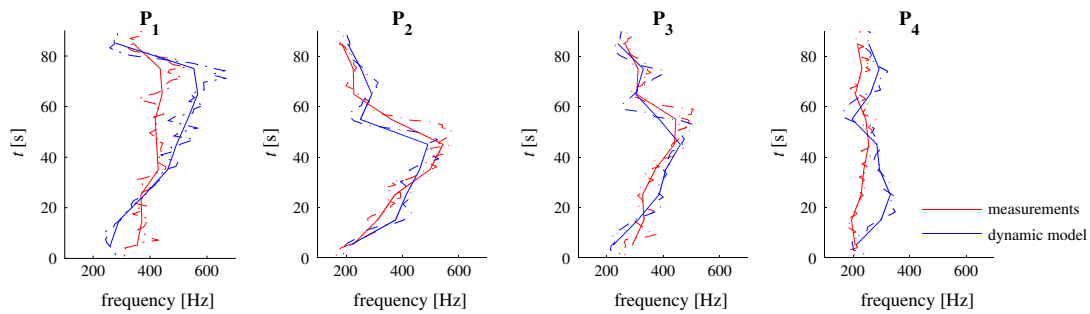


Fig. 5. Spectrum Gravity Center evolution within mean noise patterns; dotted line: 1s-evolution, solid line: 10s-evolution.

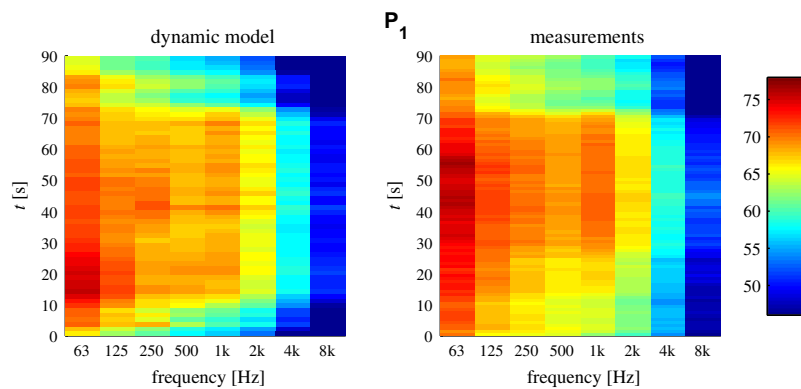


Fig. 6. Spectrum mean noise pattern at  $P_1$ , calculated by means of the dynamic model or by means of measurements.

street Vendome. This overestimation can be explained by the fact that those two contributions correspond to traffic situations where the static model dramatically overestimates real vehicle speeds. Indeed, in both situations, stops or slowing-downs of vehicles are not represented by the model.

### 3.1.3. Dynamic model

The dynamic model improves the estimation of spectrum envelopes, since it takes speed variations into account. The low frequencies emitted at slow speeds and during the acceleration phases and the 1 kHz frequencies mainly emitted at free-flow speed can thus be reproduced by the model. This improvement in the estimation of vehicles kinematics also results in an improvement of the SGC estimation: errors fall between 2% and 18%. Nevertheless, the estimation of the SGC could be improved at the points  $P_2$  and  $P_3$ , where the 63 Hz bandwidth sound level is underestimated. This error may be due to an underestimation of the background noise at those points. Finally, the accurate modeling of the part of vehicles that move at free-flow speed improves the 1 kHz bandwidth sound level estimation. It induces a precise estimation of the NR, which is “fixed” by this frequency, as it is most often the noisiest one. NR is indeed estimated with errors under 1 dB(Lin) for the points located on the main road ( $P_1$ ,  $P_2$ , and  $P_3$ ). NR estimation is not as good for the point  $P_4$ , mainly because high frequencies are underestimated. This underestimation might come from a specific propagation phenomena (the site here is large with trees close to  $P_4$ ) or from an underestimation of vehicles speed on this secondary road by the model.

### 3.2. Dynamic indicators

The dynamic modeling chain allows for the estimation of noise variations. It has been chosen to focus on noise variations that oc-

cur at the traffic cycle scale, as mentioned in Section 2.2.3.2. The Spectrum Gravity Center evolutions, which are shown in Fig. 5, and the «spectrum mean noise patterns», which are depicted for points  $P_1$ – $P_4$  on Figs. 6–9, respectively, show the main averaged spectra evolutions within traffic cycles. Note that in each figure, the time  $t = 0$  correspond to the instant when the traffic signal directly upstream the receiver turns green. Hence the figures do not show the delay between traffic signals.

- *Point  $P_1$ .* This point is located in front of a bus station and downstream of a traffic signal; see Fig. 1. The pattern extracted from measurements (see Fig. 6) clearly shows the periodicity between the high levels reached during the green<sup>4</sup> time (from  $t = 1$  s to  $t = 70$  s) and the low levels reached during the red time. Moreover, the pattern shows the increasing proportion of medium and high frequencies when the traffic signal turns green. This corresponds to the speed increase of the vehicles that pass by in front of the receiver. This tendency is reproduced by the model, although the model seems to anticipate this phenomena (see around  $t = 15$  s for the 500 Hz frequency).
- *Point  $P_2$ .* This point is located in front of the traffic signal  $T_{IV}$ ; see Fig. 1. Hence, the distinction between the green phase (from  $t = 0$  s to  $t = 50$  s) and the red phase (from  $t = 50$  s to  $t = 90$  s) is strongly pronounced; see Fig. 7. Sound levels at the 250 Hz–1 kHz bandwidth suddenly decrease when traffic signal turns red, while low frequencies remain at a high level. This variation in the pitch of sound is highlighted by the SGC, which rises during the green phase and drops during the red phase; see Fig. 5. Those pitch variations are accurately simulated by the dynamic model, since they result from speed variations reproduced by

<sup>4</sup> For interpretation of color in Figs. 1, 3, 5–9, the reader is referred to the web version of this article.



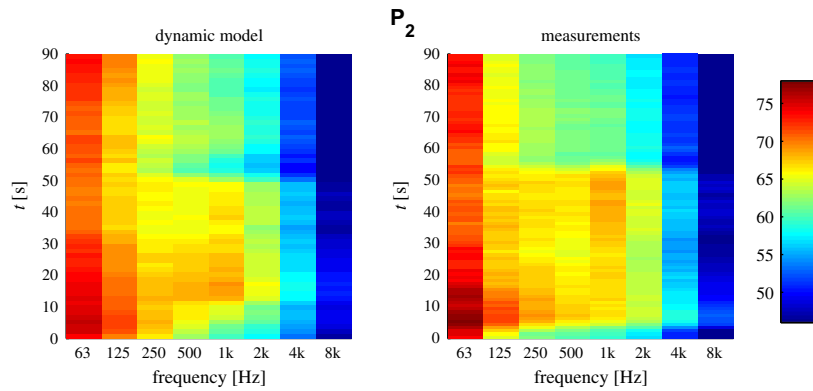


Fig. 7. Spectrum mean noise pattern at  $P_2$ , calculated by means of the dynamic model or by means of measurements.

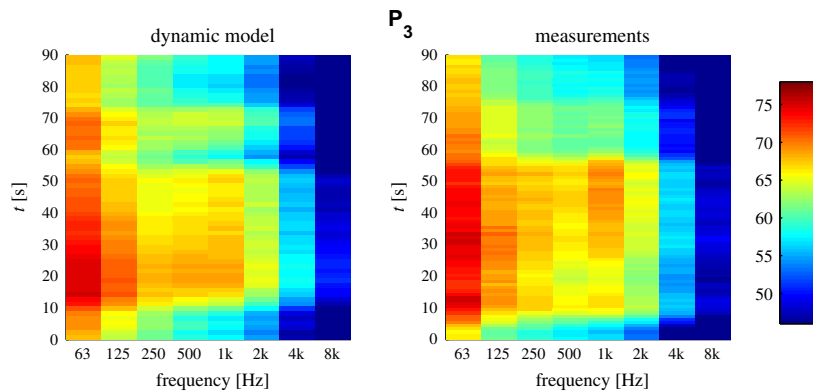


Fig. 8. Spectrum mean noise pattern at  $P_3$ , calculated by means of the dynamic model or by means of measurements.

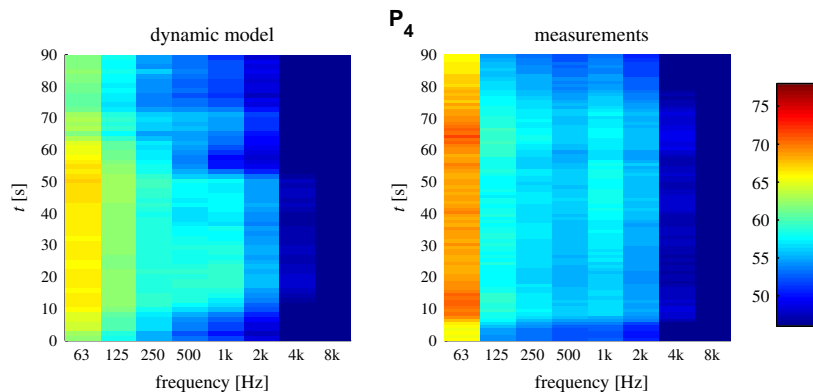


Fig. 9. Spectrum mean noise pattern at  $P_4$ , calculated by means of the dynamic model or by means of measurements.

the traffic model. However, the model slightly underestimates the 63 Hz sound levels. Nevertheless, those high 63 Hz levels may correspond to background noise and may not be directly linked to the traffic flow, as the difference between 63 Hz and 125 Hz values from measurements are very high.

- *Point  $P_3$ .* This point is located down to the traffic signal  $T_{IV}$ ; see Fig. 1. The pattern has a similar envelope as the one observed at  $P_2$ ; see Fig. 8. Nevertheless, the sound powers from 250 Hz to 1 kHz remain at a high value once the traffic signal turns red, which correspond first to the passing by of vehicles that crossed the traffic signal at the end of the cycle (from  $t = 50$  s to  $t = 60$  s), and then to the flow of the vehicles previously stored onto the perpendicular secondary streets (from  $t = 60$  s to  $t = 75$  s). More-

over, compared to  $P_2$ , the higher distance from the traffic signal makes the pitch variation evolve slower, as underlined in Fig. 5. Those patterns, which are also traffic flow dynamics, are exhibited by the simulation.

- *Point  $P_4$ .* This point is located along a perpendicular secondary street; see Fig. 1. Hence, it is less prone to high noise levels and high variations; see Fig. 9. Sound levels from 125 Hz to 2 kHz are almost invariant with time, and stay between 55 and 60 dB(Lin). However, the dynamic model cannot completely capture the spectrum mean noise pattern and still shows the shape of the pattern from the main street, probably because it underestimates noise that comes from the perpendicular street; see Section 3.1.3. Moreover, the greatest distance

from the main street also triggers a relative constant pitch; see Fig. 5. It stays at low values since 63 Hz noise levels are predominant at this point. Note that the measured 63 Hz values are surprisingly high, and are underestimated by the model. They may be due to low pitched background noise, which predominates as traffic noise is lower at this point. They may also be the result of specific propagation effects, such as multiple reflections within the street, which carry noise from the main street.

#### 4. Conclusion

Two traffic representations have been tested in this paper to estimate the sound spectrum along an urban corridor: a static one, which supposes a constant mean speed for all vehicles, and a dynamic one, which reproduces the motion of each vehicle along the network as well as their interactions. Comparison was achieved by confronting sets of model results to on-field data, collected at four points corresponding to different traffic situations: close to a bus station, in front of a traffic signal, down a traffic signal, and farther away from the corridor.

Since it is based on a coarse description of traffic flow, the static model fails in reproducing the spectra envelopes along the corridor. In particular, low frequencies sound levels are systematically underestimated, since they are mainly emitted by vehicle at slow speeds or accelerating vehicles, which are not reproduced by the static model. This could be knotty for achieving noise impact studies, especially when they involve noise reducers that often offer better performance for high frequencies than for low frequencies. Results of the static model could be improved by using speed distributions instead of a mean speed when assessing noise emissions. This could be obtained by elaborating noise emission laws that correspond to real traffic situations.

The dynamic representation outperforms the static one. Firstly, it improves the estimation of the spectra envelopes, because it is able to capture the part of slowly moving vehicles as well as the part of freely-moving vehicles. This enables a precise estimation of indicators that describe the sound spectra, such as the Spectrum Gravity Center, which approximates the pitch of the sound, and the Noise Rating value, which is deduced from the value of the noisiest octave bandwidth. Secondly, it allows for the estimation of spectra variations, since the output of the model is the 1s-sound levels evolution. Those variations are illustrated in the paper by exhibiting with a pretty good accuracy: (i) the spectrum mean noise patterns, which represent for each octave bandwidth the average evolution of sound levels within traffic signal cycles, (ii) the Spectrum Gravity Center evolution within traffic cycles. Hence, this modeling chain enables a faithful physical description of urban noise, including both sound levels and spectra variations.

To go further, a wider range of situations (two ways road, congested ring roads, different distances from the road, etc.), should be tested to clarify in which cases the dynamic traffic representation is useful. There is a strong assumption that it will be useful in every usual urban traffic situations, as it greatly improves the description of traffic characteristics. Its efficiency for situations where noise dynamics is less pronounced, such as ring roads or at greatest distance from the road, should be questioned. The dynamic traffic representation might be also useful in those situations as it can reproduce speed reductions induced by flow rates increase or stop-and-go situations, and their effects on noise spectra emitted by vehicles. Finally, a next step of this research is to couple the dynamic noise modeling chain to a perception model. This would improve the analysis of noise perception in urban area, and lead to a

global accurate tool for assessing the impact of urban traffic management policies.

#### Acknowledgements

The authors would like to thank Estelle Chevalier, for her careful reading that greatly improved the quality of the paper, and Jérôme Defrance, for providing the results of the propagation calculation. This research was partly founded by “the Région Rhône-Alpes”.

#### References

- [1] Ishima T, Hashimoto T. The impact of sound quality on annoyance caused by road traffic noise: an influence of frequency spectra on annoyance. *JSAE Rev* 2000;21(2):225–30.
- [2] Leventhall G. A review of published research on low frequency noise and its effects. Contract ref: EPG 1/2/50, Department for Environment, Food and Rural Affairs, London, UK, May 2003.
- [3] Persson K, Bjorkman M. Annoyance due to low frequency noise and the use of the dB(A) scale. *J Sound Vib* 1988;127(3):491–7.
- [4] Lim T. Correlations between deficiencies in power window systems influencing sound quality and some psychoacoustics metrics. *Appl Acoust* 2001;62:1025–47.
- [5] Lelong J, Le Duc E, Doisy S. New vehicle noise emission for French traffic noise. In: *Proceedings of inter-noise*. Ottawa (Canada); 2009.
- [6] HARMONOISE, Source modelling of road vehicles, work package 1.1. 2004: Project funded by the EC under the information society and technology (IST) programme. 52 p.
- [7] Watts G, Chandler-Wilde S, Morgan P. The combined effects of porous asphalt surfacing and barriers on traffic noise. *Appl Acoust* 1999;58:351–77.
- [8] Van Renterghem T, Botteldoren D. Reducing the acoustical facade load from road traffic with green roofs. *Build Environ* 2009;44:1081–7.
- [9] Defrance J, Jean P. Integration of the efficiency of noise barrier caps in a 3D ray tracing method. Case of a T-shaped diffracting device. *Appl Acoust* 2003;64:765–80.
- [10] Leclercq L, Lelong J. Dynamic evaluation of urban traffic noise. Adriano Alippi. In: *Proceedings of the 17th international congress on acoustics*; 2001.
- [11] De Coensel B, De muer T, Yperman I, Botteldoren D. The influence of traffic flow dynamics on urban soundscape. *Appl Acoust* 2005;66:175–94.
- [12] Oshino Y, Tsukui K, Hanabusa H, Bhaskar A, Chung E, Kuwahara M. Study on road traffic noise prediction model taking into account the citywide road network. In: *Proceedings of inter-noise*, Istanbul (Turkey); 2007. 8 p.
- [13] Can A, Leclercq L, Lelong J, Defrance J. Accounting for traffic dynamics improves noise assessment: experimental evidence. *Appl Acoust* 2009;70:821–9.
- [14] Leclercq L, Can A, Crepeaux P, Defrance J, Fournier M, Lelong J, Miegé B, Minaudier C, Olmy X, Vincent B. Dynamic prediction of urban traffic noise: a real case study (in French: «Estimation dynamique du bruit de circulation en milieu urbain: étude d'un cas réel»). *Rapport INRETS/LICIT No. 0703*. 2008. 65 p.
- [15] Can A, Leclercq L, Lelong J. Selecting noise source and traffic representations that capture urban traffic noise dynamics. *Acta Acust United Acust* 2009;95(2):259–69.
- [16] Mithra, Manuel technique. Mithra 5.0; 2002. p. 58.
- [17] Chevallier E, Can A, Nadji M, Leclercq L. Improving noise assessment at intersections by modeling traffic dynamics. *Transport Res Part D: Transport Environ* 2009;14(2):100–10.
- [18] Leclercq L. Bounded acceleration closed to fixed and moving bottlenecks. *Transport Res Part B* 2007;41(3):309–19.
- [19] Leclercq L, Chanut S, Lesort JB. Moving bottlenecks in Lighthill–Whitham–Richards model: a unified theory. *Transport Res Record: J Transport Res Board* 2004;1883:3–13.
- [20] Laval J, Leclercq L. Microscopic modeling of the relaxation phenomenon using a macroscopic lane-changing model. *Transport Res Part B* 2008;42(6):512–22.
- [21] Chevallier E, Leclercq L. Do microscopic merging models reproduce the observed priority sharing ratio in congestion? *Transport Res Part C* 2009;17:328–36.
- [22] Chevallier E, Leclercq L. A microscopic dual-regime model for single-lane roundabouts. *J Transport Eng* 2009;135(6):386–94.
- [23] Raimbault M, Lavandier C, Bérengier M. Ambient sound assessment of urban environments: field studies in two French cities. *Appl Acoust* 2003;64:1241–56.
- [24] ISO 1996-1:2003. Acoustics – description, measurement and assessment of environmental noise – part 1: basic quantities and assessment procedures.
- [25] Can A, Leclercq L, Lelong J, Defrance J. Capturing urban traffic noise dynamics through relevant descriptors. *Appl Acoust* 2008;69:1270–80.